ROBUST AUTOMATIC VOLTAGE REGULATOR DESIGN USING BODE'S IDEAL TRANSFER FUNCTION

Hanane BEKKOUCHE, Abdelfatah CHAREF

Laboratoire de Traitement de Signal, Département d'Electronique,
Faculté des Sciences de la Technologie
Université des Frères Mentouri Constantine 1, Algérie

Résumé

La commande robuste basée sur le calcul d'ordre fractionnaire gagne de plus en plus d'intérêt parmi la communauté des chercheurs du domaine de la commande. Dans cet article, une conception d'un régulateur de tension automatique (AVR) robuste basée sur le calcul d'ordre fractionnaire est présentée. La stratégie de conception du contrôleur est établi de telle sorte que la fonction de transfert en boucle ouverte du système AVR est la fonction de transfert idéale de Bode qui est très **utilisée** dans le domaine de la commande d'ordre fractionnaire en raison de sa propriété d'iso-amortissement qui est une caractéristique importante dans la robustesse. La technique de conception proposée consiste à choisir les pôles et les zéros du contrôleur pour forcer la fonction de transfert en boucle ouverte de l'AVR d'être la fonction de transfert idéale de Bode. L'idée de base et les équations de la méthode **de** conception du contrôleur sont présentées. Des simulations ont été effectuées pour tester l'efficacité et l'utilité de l'approche proposée pour la conception du contrôleur. L'analyse des performances aux variations du gain et de la constante de temps du générateur de l'AVR ont été également présentés. Des comparaisons ont été faites avec le contrôleur PID classique pour montrer la robustesse de la conception proposée par rapport aux incertitudes des paramètres du générateur.

Mots clés : *AVR, boucle idéale de Bode, les opérateurs ordre fractionnaire, le contrôleur d'ordre fractionnaire, la fonction d'approximation Rational, Robustesse.*

Abstract

Robust control based on fractional order calculus is gaining more and more interests from the control community. In this paper, a robust automatic voltage regulator (AVR) design based on fractional order calculus is presented. The controller design strategy is drawn up such that the open loop transfer function of the AVR system is the Bode's ideal transfer function that is widely used in the fractional order control domain because of its iso-damping property which is an important robustness feature. The controller design consists of choosing the poles and the zeros of the proposed controller to force the AVR open-loop transfer function to be the Bode's ideal transfer function. The basic ideas and the derived formulations of the controller design are presented. Simulations were made to test the effectiveness and the usefulness of the proposed controller design approach. Performances analysis to variations of the gain and the time constant of the generator of the AVR were also presented. Comparisons are made with PID controllers to show the robustness efficiency of the proposed design with respect to the generator parameters uncertainties.

Key words: *AVR, Bode's ideal loop, fractional order operators, fractional order control, rational function approximation, robustness*

ملخص

المراقبة القوية التي تعتمد على حساب الأس الكسري تكتسب المزيد و المزيد من الاهتمام من قبل الباحثين في ميدان المراقبة. في هذه البحث قدمنا تصميم قوي لمنظم الجهد التلقائي (AVR) يعتمد على حساب الأس الكسري. إستراتيجية تصميم المراقب وضعت لكي تكون معادلة الحلقة المفتوحة من نظام AVR هي معادلة الحلقة المفتوحة المثالية لـ BODE التي تستخدم في نطاق واسع للمراقبة ذات الأس الكسري بسبب خاصية التخامد والتي هي ميزة هامة في التقوية. تصميم المراقب تعتمد على اختيار الأقطاب و الاصفار للمراقب المقترح لإجبار معادلة الحلقة المفتوحة AVR أن تكون المعادلة المثالية لـ BODE. الأفكار الأساسية و الصيغ المشتقة قد عرضت, وقدمت التشابه لاختيار فعالية و جدوى من منهجية تصميم المراقب المقترح. وقد قدمت أيضا تحليل الكفاءة لتغيير الربح و ثابت وقت المولد لمنظم الجهد التلقائي AVR. تم إجراء مقارنات مع المراقب PID لإظهار كفاءة متانة التصميم المقترح فيما يتعلق بقضية خصائص المولد

كلمات مفتاحيه : *منظم الجهد التلقائي (AVR) ، حلقة بود المثالية، مشغل النظام الجزئي، ومراقبة النظام الجزئي، وظيفة التقريب العقلانية ، المتانة.*

Fractional order control (FOC) is a field of control theory that uses fractional order operators and systems as part of the control system design schemes. The generalization to non-integer-orders of traditional controllers or control schemes translates into more tuning parameters and more adjustable time and frequency responses of the control system, allowing the fulfillment of robust performances. In recent decades a considerable focus on FOC has been simulated by the applications of this concept in different areas of control fields [1-6].

Some early work on FOC, though without mention of the term fractional, was done by Bode who proposed an open loop transfer function to maintain stable operation of feedback amplifiers for large gain variation, nowadays known as Bode's ideal transfer function [7]. Applying Bode's idea to the position control of massive object, Tustin et al proposed a fractional order open loop transfer function in order to keep phase margin invariant to gain changes around the crossover frequency [8]. The first attempts towards the application of fractional calculus in feedback control system can be found in [9-11]. But the first who really introduced a fractional order controller was Oustaloup who developed the so-called CRONE controller and used it in various control applications [1].

Recently Podlubny, by combining the classical PID controller and the fractional calculus, proposed the fractional $PI^\lambda D^\mu$ controller, involving an integration action of order λ and differentiation action of order μ [12]. Since, many tuning techniques of the fractional $PI^\lambda D^\mu$ controller have been proposed to fulfill different control design specifications [13-20]. In [21], we can find a good tutorial on fractional calculus in controls; additionally, several typical known fractional order controllers have been presented and commented. Through the range of design techniques and applications, it is clear that FOC has become an important research topic.

In a synchronous generator, the electromechanical coupling between the rotor and the rest of the system exhibits an oscillatory behavior around the equilibrium state, following any disturbance, such as sudden change in loads. Hence, synchronous generator excitation control is one of the most important measures to enhance power system stability and to guarantee the quality of electrical power it provides.

Essentially, an automatic voltage regulator (AVR) system is a system that holds the generator terminal voltage magnitude at a specified level under normal operating conditions at various load levels [22]. Because the PID controller has a simple structure which is easy to be understood by engineers and has good performances within a wide range of operating conditions, it continues to be the main component in the AVR system. Different PID parameter tuning strategies have been reported in the literature to realize an AVR system with the best dynamic response [23-30].

More recently, fractional order $PI^\lambda D^\mu$ controller has also been proposed for the purpose of system control quality enhancement and improvement of the AVR control system [31-36]. The interest of this kind of controllers is justified by a better flexibility, since it has two more parameters, the fractional integration action order λ and the fractional differentiation action order μ. These parameters can be used to fulfill additional specifications for the design or other interesting requirements for the AVR control system.

In this paper, a control scheme to design a robust AVR system based on fractional order calculus is presented. Inspired from a recent fractional controller design technique [37], the proposed controller design strategy is drawn up such that the overall open loop transfer function of the AVR system is the Bode's ideal function that is widely used in the fractional order control domain because of its iso-damping property which is an important robustness feature.

The design technique consists of choosing the poles and the zeros of the proposed controller to force the overall open-loop transfer function of the AVR system to be the approximation of the Bode's ideal transfer function in a given frequency interval. Simulations were made to test the effectiveness and the usefulness of the proposed controller design approach. Performances analysis to variations of the gain and the time constant of the generator of the AVR were also presented. Comparisons are made with PID controllers to show the robustness efficiency of the proposed design with respect to the generator parameters uncertainties.
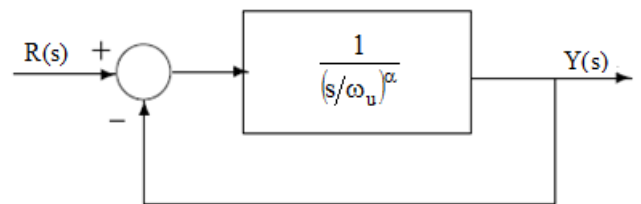
1. BODE'S IDEAL TRANSFER FUNCTION

Bode in [7] has find that the ideal open loop transfer function to design a closed loop feedback amplifier whose performance is invariant to changes in the amplifier gain is a fractional integrator with transfer function :

$$H_B(s) = \frac{1}{\left(\dfrac{s}{\omega_u}\right)^\alpha} \quad , \quad \text{for } 1 < \alpha < 2 \qquad (1)$$

where ω_u is the unity gain crossover frequency.

Known, nowadays as the Bode's ideal transfer function, this function exhibits important properties such as infinite gain margin and constant phase margin leading to the iso-damping property which is an important robustness feature for the feedback control system. This robustness has motivated some researchers to consider the unity feedback control system whose forward path transfer function is the Bode's ideal transfer function as shown in figure 1.

Figure 1 : Feedback system with Bode's ideal transfer function in the forward path

Thus, the closed-loop transfer function of the fractional order system of Fig. 1, is given by:

$$H(s) = \frac{1}{1 + \left(\dfrac{s}{\omega_u}\right)^{\alpha}} \quad , \quad \text{for } 1 < \alpha < 2 \quad (2)$$

Besides of the iso-damping property, this fractional system exhibits behavior from relaxation to oscillation. It has also been shown that all the time and frequency performances of the feedback control system of (2) whose open loop is the Bode's ideal function of (1) depends on the parameters α and ω_u only [38-39]. For these raisons, it has been considered as a control reference system in lot of work in the literature.

1.1. Fractional Order Integrator

The analog transfer function of the fractional order integrator is represented in the frequency domain by the following irrational function:

$$H_I(s) = \frac{1}{s^{\alpha}} \quad , \quad \text{for } \alpha > 0 \quad (3)$$

In a given a frequency band of interest $[\omega_L, \omega_H]$ with a given integer number N, a chosen error of approximation in dB y and a chosen frequency ω_c such that $\omega_c < \omega_L$, the rational function approximation of the fractional order integrator $H_I(s)$ can be expressed as follows [16, 40]:

$$H_I(s) = \frac{1}{s^{\alpha}} = \left(\frac{1}{s^{N_1}}\right)\left(\frac{1}{s^{(\alpha - N_1)}}\right)$$

$$\approx \left(\frac{1}{\left[\prod\limits_{i=-N_1}^{-1}(p_i)\right]\left[\prod\limits_{i=-N_1}^{-1}(1+s/p_i)\right]}\right)\left(\frac{1}{(\omega_c)^{(\alpha-N_1)}}\frac{\prod\limits_{i=0}^{N}(1+s/z_i)}{\prod\limits_{i=0}^{N}(1+s/p_i)}\right) \quad (4)$$

$$= \frac{1}{\left[\prod\limits_{i=-N_1}^{-1}(p_i)\right]}\frac{1}{(\omega_c)^{(\alpha-N_1)}}\frac{\prod\limits_{i=0}^{N}(1+s/z_i)}{\prod\limits_{i=-N_1}^{N}(1+s/p_i)}$$

with N_1 is the integer part of the fractional order α and the poles p_i and the zeros z_i are : $p_i = p_0(ab)^i$ (for i = -N₁…,-1,0,1,…,N) and $z_i = ap_0(ab)^i$ (for i = 0,1,…,N); where the approximation parameters a, b and p_0 are given as follows [16, 40] :

$$a = 10^{\left[\frac{y}{10(1-\alpha+N_1)}\right]}, b = 10^{\left[\frac{y}{10(\alpha-N_1)}\right]}, p_0 = \omega_c 10^{\left[\frac{y}{20(\alpha-N_1)}\right]}$$

1.2. Oscillation Fractional Order System

The oscillation fractional order system is defined by the following transfer function [41]:

$$H(s) = \frac{1}{[1 + (\tau_0 s)^{\alpha}]} \quad (5)$$

where τ_0 is the characteristic relaxation time and $1 < \alpha < 2$.

In a given frequency band of interest $[0, \omega_H]$, the transfer function of the oscillation fractional order system of (5) can be approximated by a rational function as follows [41] :

$$H(s) \cong \frac{\prod\limits_{i=0}^{N}\left(1 + \dfrac{s}{z_i}\right)}{\prod\limits_{i=0}^{N}\left(1 + \dfrac{s}{p_i}\right)}\frac{1}{\left[(\tau_0 s)^2 + 2\zeta(\tau_0 s) + 1\right]} \quad (6)$$

where the parameter ζ, the zeros z_i (i=0,1,…,N) and the poles p_i (i=0,1,…,N) are given by :

$$\zeta = \sqrt{\frac{[1 + \cos(\frac{\pi}{2}\alpha)]}{2^{\alpha-1}}} \quad , \quad z_i = z_0(ab)^i \quad ,$$

$$p_i = az_0(ab)^i$$

The approximation parameters a, b, z_0 and N are given as follows [41]:

$$a = 10^{\left[\frac{\varepsilon}{10[1-(2-\alpha)]}\right]}, \quad b = 10^{\left[\frac{\varepsilon}{10(2-\alpha)}\right]}, \quad z_0 = \frac{1}{\tau_0}10^{\left[\frac{\varepsilon}{20(2-\alpha)}\right]}$$

$$\text{and } N = \text{Integer}\left[\frac{\log\left(\dfrac{\omega_{max}}{z_0}\right)}{\log(ab)}\right] + 1$$

where the parameters ω_{max} is such that $\omega_{max} \gg \omega_H$ and ε is a given error of approximation in dB.

By partial fraction expansion the rational function of (6) can be rewritten as **[41]:**

$$H(s) \cong \sum\limits_{i=0}^{N}\frac{k_i}{\left(1 + \dfrac{s}{p_i}\right)} + \frac{As + B}{(\tau_0 s)^2 + 2\zeta(\tau_0 s) + 1} \quad (7)$$

where the residues k_i (i=0,1, …, N), the constants A and B are :

$$k_i = \frac{\prod\limits_{j=0}^{N}\left[1 - a(ab)^{(i-j)}\right]}{\prod\limits_{\substack{j=0 \\ i\neq j}}^{N}\left[1 - (ab)^{(i-j)}\right]}\left\{\frac{1}{(\tau_0 p_i)^2 - 2\zeta(\tau_0 p_i) + 1}\right\},$$

$$B = 1 - \sum_{i=0}^{N} k_i \quad \text{and} \quad A = -\tau_0^2 \sum_{i=0}^{N} k_i p_i$$

Using the inverse Laplace transform of (7), we will get:

$$h(t) = \sum_{i=0}^{N} k_i p_i \exp(-p_i t) + C \exp\left(-\frac{\zeta}{\tau_0} t\right) \sin\left(\frac{\sqrt{1-\zeta^2}}{\tau_0} t + \Phi\right) \quad (8)$$

where the constants C and Φ are :

$$C = \sqrt{\frac{A^2 - 2AB\zeta\tau_0 + (B\tau_0)^2}{(\tau_0)^4(1-\zeta^2)}} \; ,$$

$$\Phi = \text{arctg}\left(\frac{A\sqrt{1-\zeta^2}}{B\tau_0 - A\zeta}\right)$$

Let us consider the following transfer function:

$$H_1(s) = H(s)\frac{1}{s} \cong \sum_{i=0}^{N} \frac{k_i}{\left(1+\frac{s}{p_i}\right)}\frac{1}{s} + \frac{As+B}{(\tau_0 s)^2 + 2\zeta(\tau_0 s) + 1}\frac{1}{s} \quad (9)$$

Then, using the inverse Laplace transform of (9), we will get:

$$h_1(t) = 1 - \sum_{i=0}^{N} k_i \exp(-p_i t)$$

$$+ C\tau_0 \exp\left(-\frac{\zeta}{\tau_0}t\right)\sin\left(\frac{\sqrt{1-\zeta^2}}{\tau_0}t + \Phi - \Phi_1\right) \quad (10)$$

where the constant Φ_1 is : $\Phi_1 = \text{arctg}\left(\frac{\sqrt{1-\zeta^2}}{-\zeta}\right)$

2. DESCRIPTION OF THE AVR MODEL

The mathematical model of the AVR system used in this work is a linear model which takes into account the major time constants and ignores the saturation or other nonlinearities. The linear and simplified AVR system comprises four main components, namely amplifier, exciter, generator, and sensor. The transfer functions of these components including limits of their parameters are given as follows [22], [24-26]:

$$\begin{cases} \text{Amplifier:} & G_a(s) = \frac{K_a}{1+\tau_a s} \; , \; 10 \le K_a \le 40 \qquad 0.02s \le \tau_a \le 0.1s \\[2mm] \text{Exciter:} & G_e(s) = \frac{K_e}{1+\tau_e s} \; , \; 1 \le K_e \le 10 \qquad 0.4s \le \tau_e \le 1.0s \\[2mm] \text{Generator:} & G_g(s) = \frac{K_g}{1+\tau_g s} \; , \; 0.7 \le K_g \, (\text{depends on load}) \le 1.0 \quad 1.0s \le \tau_g \le 2.0s \\[2mm] \text{Sensor:} & G_s(s) = \frac{K_s}{1+\tau_s s} \; , \; K_s = 1 \qquad 0.001s \le \tau_s \le 0.06s \end{cases} \quad (11)$$

The block diagram of the AVR system in closed loop with a controller C(s) and the transfer functions of the amplifier, exciter, generator and sensor is given in figure 2.
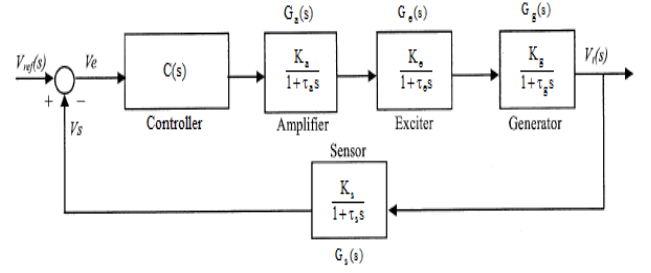
Figure 2 : block diagram of the AVR system in closed loop with a controller C(s)

The open loop transfer function G(s) of the AVR system of Fig. 2, is given as:

$$G(s) = C(s) G_p(s) \quad (12)$$

where C(s) is the controller's transfer function and $G_p(s)$ is a transfer function given as:

$$G_p(s) = G_a(s)G_e(s)G_g(s)G_s(s) = \frac{K_a K_e K_g K_s}{(1+\tau_a s)(1+\tau_e s)(1+\tau_g s)(1+\tau_s s)} \quad (13)$$

$$G_p(s) = \frac{K_a K_e K_g K_s}{\left(1+\frac{s}{\omega_1}\right)\left(1+\frac{s}{\omega_2}\right)\left(1+\frac{s}{\omega_3}\right)\left(1+\frac{s}{\omega_4}\right)} \quad (14)$$

where

$$\left(\omega_1 = \frac{1}{\tau_g}\right) < \left(\omega_2 = \frac{1}{\tau_e}\right) < \left(\omega_3 = \frac{1}{\tau_a}\right) < \left(\omega_4 = \frac{1}{\tau_s}\right)$$

are the poles of $G_p(s)$.

3. PROPOSED AVR SYSTEM DESIGN METHOD

In this work, the objective of the projected AVR system is to design a controller C(s) which will guarantee that the open loop transfer function G(s) = C(s) $G_p(s)$ of (12) behaves, in a frequency range [ω_L, ω_H] around a given frequency ω_u, as the Bode's ideal function. Hence, we will have:

$$G(s) = C(s) G_p(s) \cong \frac{1}{\left(\frac{s}{\omega_u}\right)^\alpha} \quad (15)$$

where α is a number such that $1 < \alpha < 2$ and ω_u is a positive real number.

It has been shown that the time and frequency performances of the unity feedback control whose open loop is the Bode's ideal function of (15) depend on the parameters α and ω_u [38-39]. Then, the dynamic performance requirements of the projected AVR system have to be translated in terms of α and ω_u. If the CRONE controller design technique was used the controller's transfer function C(s) will be given as [1] :

$$C(s) = \frac{1}{G_p(s)} \frac{1}{\left(\dfrac{s}{\omega_u}\right)^\alpha} \quad , \text{ for } 1 < \alpha < 2 \qquad (16)$$

But, in this context, the proposed controller $C(s)$ will be designed in a different way than the one proposed by the CRONE controller of (16). Once the two parameters α and ω_u are chosen based on the dynamic performance requirements of the projected AVR system, the frequency band of interest $[\omega_L, \omega_H]$ around ω_u where the open loop transfer function $G(s)$ of the AVR system approximates the Bode's ideal function of (15) is given as $[\omega_L = \omega_u/\beta, \omega_H = \beta\omega_u]$ for $\beta > 1$.

In section 2.1, we have presented the approximation by a rational function, in a given frequency band of interest $[\omega_L, \omega_H]$, of the fractional order integrator.

Hence, from (4) the Bode's ideal function of (15) can be approximated as:

$$G(s) = C(s)\,G_p(s) = \frac{1}{\left(\dfrac{s}{\omega_u}\right)^\alpha}$$

$$\cong \frac{(\omega_u)^\alpha}{[p_{-1}]\left[(\omega_c)^{(\alpha-1)}\right]} \frac{\displaystyle\prod_{i=0}^{N}(1 + s/z_i)}{\displaystyle\prod_{i=-1}^{N}(1 + s/p_i)} \qquad (17)$$

where p_i ($i = -1\ldots,-1,0,1,\ldots,N$) and z_i ($i = 0,1,\ldots,N$) are the poles and zeros of the approximation. The controller new design technique is based on the manipulation of the poles p_i of the approximation of the fractional order integrator of (17) such that four of these poles are almost equal to the poles ω_1, ω_2, ω_3 and ω_4 of $G_p(s)$ of (14). This pole manipulation can be easily done by choosing the right approximation parameters given in section 2.1 by a trial and error method. After doing so, the above rational function can be decomposed in two parts as:

$$G(s) = C(s)\,G_p(s) = \frac{1}{\left(\dfrac{s}{\omega_u}\right)^\alpha}$$

$$\cong \frac{(\omega_u)^\alpha}{[p_{-1}]\left[(\omega_c)^{(\alpha-1)}\right]} \frac{\displaystyle\prod_{i=0}^{N}(1 + s/z_i)}{\displaystyle\prod_{i=-1}^{N}(1 + s/p_i)}$$

$$= \left[K_c \frac{\displaystyle\prod_{i=0}^{N}\left(1 + \dfrac{s}{z_i}\right)}{\displaystyle\prod_{\substack{i=-1 \\ i\neq j_1, i\neq j_2 \\ i\neq j_3, i\neq j_4}}^{N}\left(1 + \dfrac{s}{p_i}\right)}\right]\left[\frac{K_p}{\left(1 + \dfrac{s}{p_{j_1}}\right)\left(1 + \dfrac{s}{p_{j_2}}\right)\left(1 + \dfrac{s}{p_{j_3}}\right)\left(1 + \dfrac{s}{p_{j_4}}\right)}\right]$$

$$(18)$$

where $K_p = K_a K_e K_g K_s$, $\quad K_c = \dfrac{(\omega_u)^\alpha}{(K_p)[p_{-1}]\left[(\omega_c)^{(\alpha-1)}\right]}$

and the poles p_{j1}, p_{j2}, p_{j3} and p_{j4}, are almost equal to the poles ω_1, ω_2, ω_3 and ω_4, of $G_p(s)$ of (14), respectively, with $-1 \leq j_1 < j_2 < j_3 < j_4 \leq N$. Because we have forced the right part of the above equation to be almost equal to the function $G_p(s)$; then the controller's transfer function $C(s)$ is given as :

$$C(s) = \left[K_c \frac{\displaystyle\prod_{i=0}^{N}\left(1 + \dfrac{s}{z_i}\right)}{\displaystyle\prod_{\substack{i=-1 \\ i\neq j_1, i\neq j_2 \\ i\neq j_3, i\neq j_4}}^{N}\left(1 + \dfrac{s}{p_i}\right)}\right] \qquad (19)$$

In this design method, $C(s)$ must be causal. But as we can see from the controller's transfer function $C(s)$ of (19) there is $(N+1)$ zeros and $(N-2)$ poles. Then to guarantee its causality we must add at least three poles such that they will have no effect on the design in the given frequency band $[\omega_L, \omega_H]$ around the given crossover frequency ω_u. In this context the three poles are added after the last pole p_N of the approximation by a rational function of the fractional order integrator of (17). So, the three added poles are given as :

$$p_{N+1} = p_0(ab)^{(N+1+\delta)}, \ p_{N+2} = p_{N+1}(ab) \text{ and }$$
$$p_{N+3} = p_{N+2}(ab) \qquad (20)$$

where δ is a positive real number chosen to ameliorate the approximation of the fractional order integrator $\left(\dfrac{s}{\omega_u}\right)^{-\alpha}$ of (17). Hence, the final controller's transfer function $C(s)$ will be :

$$C(s) = \left[K_c \frac{\displaystyle\prod_{i=0}^{N}\left(1 + \dfrac{s}{z_i}\right)}{\displaystyle\prod_{\substack{i=-1 \\ i\neq j_1, i\neq j_2 \\ i\neq j_3, i\neq j_4}}^{N}\left(1 + \dfrac{s}{p_i}\right)}\right]\left[\frac{1}{\displaystyle\prod_{i=N+1}^{N+3}\left(1 + \dfrac{s}{p_i}\right)}\right] \qquad (21)$$

From figure 2, the closed loop transfer function $G_c(s)$ of the AVR system is given as:

$$G_c(s) = \frac{V_t(s)}{V_{ref}(s)} = \frac{C(s)\,G_a(s)\,G_e(s)\,G_g(s)}{1 + C(s)\,G_a(s)\,G_e(s)\,G_g(s)\,G_s(s)} \qquad (22)$$

From (12) and (13) we have :

$$G(s) = C(s)\,G_p(s) = C(s)\,G_a(s)\,G_e(s)\,G_g(s)\,G_s(s);$$

so, we will get:

$$G_c(s) = \frac{V_t(s)}{V_{ref}(s)} = \frac{G(s)/G_s(s)}{1+G(s)} = \left[\frac{G(s)}{1+G(s)}\right]\left[\frac{1}{K_s} + \frac{\tau_s}{K_s}s\right] \quad (23)$$

$$= \frac{1}{K_s}\left[\frac{G(s)}{1+G(s)}\right] + \frac{\tau_s}{K_s}s\left[\frac{G(s)}{1+G(s)}\right]$$

Now, for $v_{ref}(t) = u(t) =$ the unit step, $V_{ref}(s) = 1/s$; we will have :

$$V_t(s) = \frac{1}{K_s}\left[\frac{G(s)}{1+G(s)}\right]\left(\frac{1}{s}\right) + \frac{\tau_s}{K_s}s\left[\frac{G(s)}{1+G(s)}\right]\left(\frac{1}{s}\right) \quad (24)$$

$$= \frac{\tau_s}{K_s}\left[\frac{G(s)}{1+G(s)}\right] + \frac{1}{K_s}\left[\frac{G(s)}{1+G(s)}\right]\left(\frac{1}{s}\right)$$

Then the step response of the AVR system is given as follows:

$$v_t(s) = \frac{\tau_s}{K_s}L^{-1}\left\{\frac{G(s)}{1+G(s)}\right\} + \frac{1}{K_s}L^{-1}\left\{\frac{G(s)}{1+G(s)}\frac{1}{s}\right\} \quad (25)$$

Theoretically, $G(s) = \dfrac{1}{\left(\dfrac{s}{\omega_u}\right)^\alpha}$, for $1 < \alpha < 2$, then we have :

$$\left[\frac{G(s)}{1+G(s)}\right] = \frac{1}{1+\left(\dfrac{s}{\omega_u}\right)^\alpha} \quad (26)$$

So, in this case, the ideal step response of the closed loop AVR system is given as follows:

$$v_t(t) = \frac{\tau_s}{K_s}L^{-1}\left\{\frac{1}{1+\left(\dfrac{s}{\omega_u}\right)^\alpha}\right\} + \frac{1}{K_s}L^{-1}\left\{\frac{1}{1+\left(\dfrac{s}{\omega_u}\right)^\alpha}\frac{1}{s}\right\} \quad (27)$$

$$= \frac{\tau_s}{K_s}h(t) + \frac{1}{K_s}h_1(t)$$

where, for $\tau_0 = 1/\omega_u$, $h(t)$ and $h_1(t)$ are the impulse and step responses of the oscillation fractional order system of (5) given in (8) and (10), respectively, as:

$$h(t) = \sum_{i=0}^{N}k_i p_i \exp(-p_i t) + C\exp(-\omega_u \zeta t)\sin\left(\omega_u\left(\sqrt{1-\zeta^2}\right)t + \Phi\right) \quad (28)$$

$$h_1(t) = 1 - \sum_{i=0}^{N}k_i \exp(-p_i t) + \left(\frac{C}{\omega_u}\right)\exp(-\omega_u \zeta t)\sin\left(\omega_u\left(\sqrt{1-\zeta^2}\right)t + \Phi - \Phi_1\right) \quad (29)$$

4. SIMULATIONS RESUSLTS AND COMPARISONS

4.1. Controller design for the AVR system

The block diagram of the practical AVR system in closed loop with nominal values of the parameters of the transfer functions of the amplifier, exciter, generator and sensor is given in figure 3, [23-25]. This AVR system model will be used in this work to verify the efficiency of the proposed controller. Only the variations of the gain and the time constant of the generator will be considered for the performances and robustness analysis because we want that the AVR system to hold the generator terminal voltage magnitude at a specified level under normal operating conditions at various load levels.
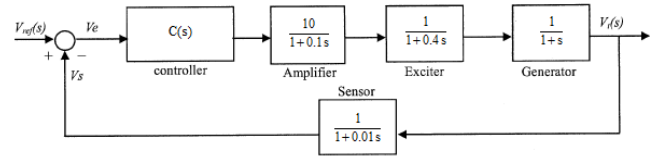
Figure 3 : block diagram of the practical AVR system

The transfer function $G_p(s)$ of the above AVR system is given as:

$$G_p(s) = \frac{10}{(1+0.1s)(1+0.4s)(1+s)(1+0.01s)}$$

$$= \frac{10}{(1+\dfrac{s}{1.0})(1+\dfrac{s}{2.5})(1+\dfrac{s}{10.0})(1+\dfrac{s}{100.0})} \quad (30)$$

The goal of the projected AVR system is to design the controller $C(s)$ which will guarantee that the open loop transfer function $G(s) = C(s) G_p(s)$ of the AVR system is the Bode's ideal transfer function $G_B(s)$ given as follows:

$$G(s) = C(s) G_p(s) = G_B(s) = \frac{1}{\left(\dfrac{s}{\omega_u}\right)^\alpha} \quad (31)$$

The dynamic performance requirements of the projected AVR system are: a small settling time t_s and a small or no overshoot Os (%) [23-25]. These requirements have to be translated in terms of the two parameters α and ω_u of the Bode's ideal transfer function. The values of the parameters α and ω_u can be estimated from the time characteristics (overshoot and settling time) of the oscillation fractional order system of (5) given in [38] using the Mittag-leffler approach or in [39] using the approach of [41]. The above dynamic performance requirements can be satisfied for $\alpha = 1.1$ and $\omega_u = 40$ rad/s.

Hence, the open loop transfer function $G(s)$ of the AVR system will be:

$$G(s) = C(s) G_p(s) = G_B(s) = \frac{1}{\left(\dfrac{s}{40}\right)^{1.1}} \quad (32)$$

So, from section (2.1), the fractional integrator of (32) can be approximated as:

$$C(s)\ G_p(s) = \frac{1}{\left(\dfrac{s}{40}\right)^{1.1}} \cong \frac{(40)^{1.1}}{(p_{-1})(\omega_c)^{0.1}} \frac{\displaystyle\prod_{i=0}^{N}\left(1+\dfrac{s}{z_i}\right)}{\displaystyle\prod_{i=-N_1}^{N}\left(1+\dfrac{s}{p_i}\right)} \quad (33)$$

For the unity gain crossover frequency $\omega_u = 40$ rad/s, the frequency band of interest around ω_u is $[\omega_L, \omega_H] = [\omega_u/10, 10\omega_u] = [4$ rad/s, 400 rad/s$]$. Also, for N=10, y = 0.2948 dB, $\omega_c = 0.3624$ rad/s and $N_1=1$, the approximation parameters a, b, and p_0 are: a = 1.0783, b= 1.9716, $p_0 = 0.5088$. Then, the poles and zeros of (33) are :

$p_i = p_0(ab)^i = 0.5088(2.1260)^i$ (for i = -1,0,1,…,10) and

$z_i = ap_0(ab)^i = 0.5486(2.1260)^i$ (for i = 0,1,…,10).

Hence, the open loop transfer function G(s) = C(s) G_p(s) of the AVR system will be:

$$G(s) = C(s)\ G_p(s) = \frac{1}{\left(\dfrac{s}{40}\right)^{1.1}}$$

$$\cong (267.4904)\frac{\displaystyle\prod_{i=0}^{10}\left(1+\dfrac{s}{0.5486(2.1260)^i}\right)}{\displaystyle\prod_{i=-1}^{10}\left(1+\dfrac{s}{0.5088(2.1260)^i}\right)} \quad (34)$$

By choosing the right parameters ω_c and y, we have made the poles $p_1=1.0818$, $p_2=2.3$, $p_4=10.3957$ and $p_7=99.8951$ of the approximation of the fractional integrator of (33) almost equal to the poles $\omega_1=1.0$, $\omega_2=2.5$, $\omega_3=10.0$ and $\omega_4=100.0$ of G_p(s), respectively. So, the rational function of the right hand side of (34) can be decomposed in two parts as:

$$C(s)G_p(s) = \left[(26.7490)\frac{\displaystyle\prod_{i=0}^{10}\left(1+\dfrac{s}{0.5486(2.1260)^i}\right)}{\displaystyle\prod_{\substack{i=-1 \\ i\neq 1, i\neq 2 \\ i\neq 4, i\neq 7}}^{10}\left(1+\dfrac{s}{0.5088(2.1260)^i}\right)}\right] \quad (35)$$

$$\left[\frac{10.00}{\left(1+\dfrac{s}{1.0818}\right)\left(1+\dfrac{s}{2.3000}\right)\left(1+\dfrac{s}{10.3957}\right)\left(1+\dfrac{s}{99.8951}\right)}\right]$$

Because the right hand side of the above equation is almost equal to the function G_p(s), the left hand side is then the controller's transfer function. Therefore, C(s) is given as:

$$C(s) = \left[(26.7490)\frac{\displaystyle\prod_{i=0}^{10}\left(1+\dfrac{s}{0.5486(2.1260)^i}\right)}{\displaystyle\prod_{\substack{i=-1 \\ i\neq 1, i\neq 2 \\ i\neq 4, i\neq 7}}^{10}\left(1+\dfrac{s}{0.5088(2.1260)^i}\right)}\right] \quad (36)$$

The controller's transfer function C(s) of (36) is not causal because it has 11 zeros and 8 poles. To guarantee its causality we must add at least three poles such that they will have no effect on the controller's design.

In this context, the three poles which will be added after the last pole p_{10} of (36) are given as : $p_{11}=0.5088(2.1260)^{(11+\delta)}$, $p_{12}=(2.1260)p_{11}$ and $p_{13}=(2.1260)p_{12}$

where δ is a positive real number given by $\delta = 3.43$. This number is chosen to ameliorate the approximation of the fractional order integrator of (34), especially its phase.

Finally, the designed controller's transfer function C(s) will be:

$$C(s) = \left[(26.7490)\frac{\displaystyle\prod_{i=0}^{10}\left(1+\dfrac{s}{0.5486(2.1260)^i}\right)}{\displaystyle\prod_{\substack{i=-1 \\ i\neq 1, i\neq 2 \\ i\neq 4, i\neq 7}}^{10}\left(1+\dfrac{s}{0.5088(2.1260)^i}\right)}\right] \quad (37)$$

$$\left[\frac{1}{\displaystyle\prod_{i=11}^{13}\left(1+\dfrac{s}{0.5088(2.1260)^{(3.43+i)}}\right)}\right]$$

Hence, the open loop transfer function G(s) = C(s) G_p(s) is given as:

$$G(s) = \left[\frac{(26.7490)\displaystyle\prod_{i=0}^{10}\left(1+\dfrac{s}{0.5486(2.1260)^i}\right)}{\displaystyle\prod_{\substack{i=-1 \\ i\neq 1, i\neq 2 \\ i\neq 4, i\neq 7}}^{10}\left(1+\dfrac{s}{0.5088(2.1260)^i}\right)\displaystyle\prod_{i=11}^{13}\left(1+\dfrac{s}{0.5088(2.1260)^{(3.43+i)}}\right)}\right]$$

$$\left[\frac{10}{\left(1+\dfrac{s}{1.0}\right)\left(1+\dfrac{s}{2.5}\right)\left(1+\dfrac{s}{10.0}\right)\left(1+\dfrac{s}{100.0}\right)}\right]$$
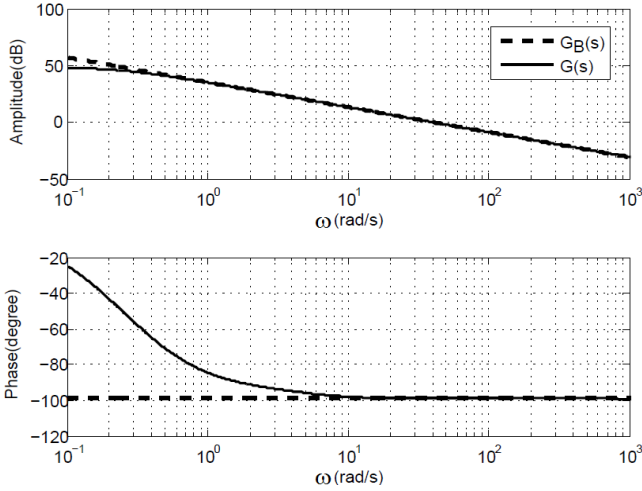
$$(38)$$

Figure 4, shows the Bode plots of the open loop transfer function G(s) of (38) and the Bode's ideal function

$$G_B(s) = \left(\frac{s}{40}\right)^{-1.1} \text{ of (32)}.$$

From Fig. 4, we can easily see that the unity gain crossover frequency is $\omega_u= 40$ rad/s and around it the slope is exactly -20(1.1) = -22.00 dB/dec and the phase is - (1.1) $90° = -99.00°$.

This means that around the unity gain crossover frequency $\omega_u= 40$ rad/s the open loop transfer function G(s) of (38) behaves as the Bode's ideal function

$$G_B(s) = \left(\frac{s}{40}\right)^{-1.1} \text{ of (32). So, this result shows the}$$

accuracy of the phase's flatness around the unity gain crossover frequency $\omega_u= 40$ rad/s.

Figure 4 : Bode plots of the open loop function G(s) and the Bode's ideal function $G_B(s)$

From Figure 3, the parameters K_s and τ_s of the sensor are $K_s=1$ and $\tau_s=0.01$, So, the closed loop transfer function $G_c(s)$ of the AVR system of (23) is given as:

$$G_c(s) = \frac{V_t(s)}{V_{ref}(s)} = \left[\frac{G(s)}{1+G(s)}\right] + 0.01s\left[\frac{G(s)}{1+G(s)}\right] \quad (39)$$

and the terminal voltage step response of the closed loop AVR system is :

$$v_t(t) = L^{-1}\left\{\frac{G(s)}{1+G(s)}\frac{1}{s}\right\} + 0.01 L^{-1}\left\{\frac{G(s)}{1+G(s)}\right\} \quad (40)$$

where G(s) is the open loop transfer function of the AVR system of (38).

Theoretically, we have $G(s) = G_B(s) = \left(\frac{s}{40}\right)^{-1.1}$, so from (39) the ideal closed loop transfer function $G_{Bc}(s)$ of the AVR system is given as:

$$G_{Bc}(s) = \frac{V_t(s)}{V_{ref}(s)} = \left[\frac{1}{1+\left(\frac{s}{40}\right)^{1.1}}\right] + 0.01s\left[\frac{1}{1+\left(\frac{s}{40}\right)^{1.1}}\right] \quad (41)$$

and from (27), the ideal terminal voltage step response of the closed loop AVR system is:

$$v_t(t) = h_1(t) + 0.01h(t) \quad (42)$$

where the functions h(t) and $h_1(t)$ of (28) and (29), respectively, are obtained using the approximation technique of [41].

In the frequency band $[0, \omega_H] = [0, 1600$ rad/s] and for an approximation error $\varepsilon = 0.5$ dB, the approximation parameters given in section (2.2) are: $\zeta = 0.8871$, $\omega_{max} = 2000$ rad/s, a = 3.1622, b = 1.1364, $z_0 = 42.642$, $p_0 = 134.846$, N = 6, A= 0.0243, B = 1.0546, C = 1.0576, $\Phi = 1.1656$, $\Phi_1 = 2.6620$. So, for i = 0, 1, …, 6, we can get :

$$p_i = 134.846(3.5938)^i$$

$$k_i = \frac{\prod_{j=0}^{6}\left[1 - 3.1622(3.5938)^{(i-j)}\right]}{\prod_{\substack{j=0 \\ i \neq j}}^{6}\left[1 - (3.5938)^{(i-j)}\right]}$$

$$\left\{\frac{1}{\left[3.3711(3.5938)^i\right]^2 - \left[5.9815(3.5938)^i\right] + 1}\right\}$$

Then, the functions h(t) and $h_1(t)$ are:

$$h(t) = \sum_{i=0}^{6} k_i 134.846(3.5938)^i \exp\left(-134.846(3.5938)^i t\right)$$
$$+ 1.0576\exp\left(-35.4840t\right)\sin\left(18.4575t + 1.1656\right)$$

$$h_1(t) = 1 - \sum_{i=0}^{6} k_i \exp\left(-134.846(3.5938)^i t\right)$$
$$+ 42.3027\exp\left(-35.4840t\right)\sin\left(18.4575t - 1.4964\right)$$

Figure 5, shows the Bode plots of the closed loop transfer functions $G_c(s)$ of (39) and the ideal closed loop transfer function $G_{Bc}(s)$ of the AVR system of (41). Fig. 6, shows also the terminal voltage step responses of the closed loop AVR system of (40) with the proposed controller and of the ideal terminal voltage step response of (42).
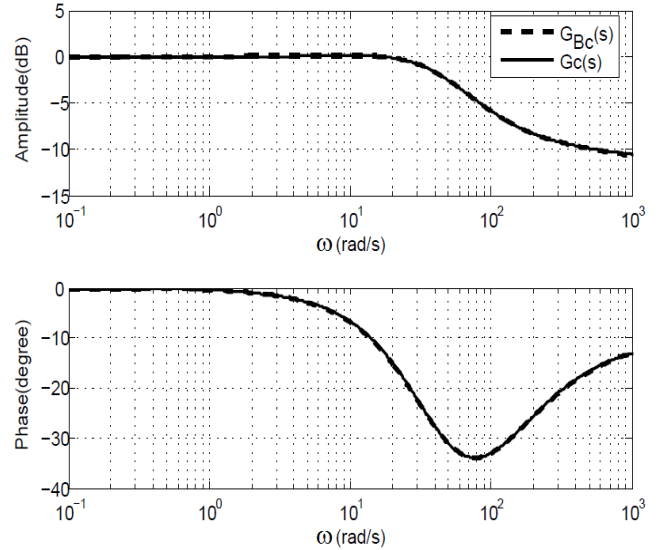

Figure 5 : Bode plots of the closed loop transfer function $G_c(s)$ and the ideal closed loop transfer function $G_{Bc}(s)$

From figure 5, we can easily see that around the unity gain crossover frequency $\omega_u = 40$ rad/s the amplitudes and the phases of the closed loop transfer function $G_c(s)$ and the ideal closed loop transfer function $G_{Bc}(s)$ of the AVR system of are quiet overlapping. Then, this result shows the effectiveness of the proposed controller design strategy.

From figure 6, we can also see that the two terminal voltage step responses are almost the same. So, the designed closed loop AVR system with the proposed controller behaves as the ideal closed loop AVR system whose closed loop transfer function is $G_{Bc}(s)$.

We can also note that the proposed controller produces a very small settling time with a very small overshoot and steady state error.
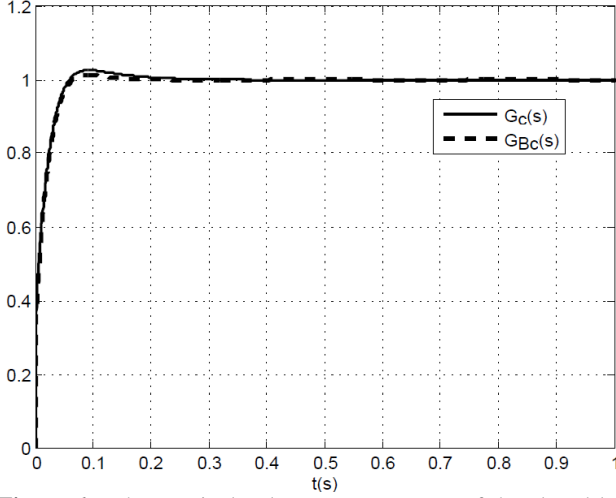
Figure 6 : The terminal voltage step response of the closed loop AVR system with the proposed controller and the ideal terminal voltage step response

4.2. performance comparison and robustness analysis

In this section, we will compare the performances as well as the robustness with respect to the variations of the gain K_g and the time constant τ_g of the generator of the proposed AVR system design to the results of the designed AVR system of [25] using a classical PID controller where a chaotic optimization approach based on Lozi map has been used in the tuning of the parameters of the PID controller.

In this comparison, we have used the same dynamic performance requirements adopted in [25]. Using the same nominal values of the parameters of the transfer functions of the amplifier, exciter, generator and sensor of figure 3, the designed PID controller with the optimized gains for the AVR system is given as [25]:

$$C_{PID}(s) = K_P + \frac{K_I}{s} + K_D s = 0.622 + \frac{0.453}{s} + 0.218s \quad (43)$$

Then, the open loop transfer function $G_{PID}(s) = C_{PID}(s) G_p(s)$ is given as:

$$G_{PID}(s) = \left[\frac{2.18s^2 + 6.22s + 4.53}{s(1 + \frac{s}{1.0})(1 + \frac{s}{2.5})(1 + \frac{s}{10.0})(1 + \frac{s}{100.0})} \right] \quad (44)$$

In this case, the closed loop transfer function $G_{PIDc}(s)$ of the AVR system is:

$$G_{PIDc}(s) = \frac{V_t(s)}{V_{ref}(s)} = \left[\frac{G_{PID}(s)}{1 + G_{PID}(s)} \right] + 0.01s \left[\frac{G_{PID}(s)}{1 + G_{PID}(s)} \right] \quad (45)$$

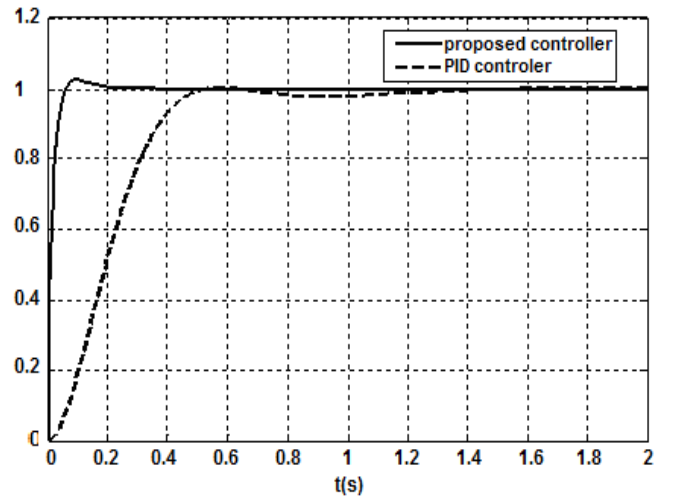And the step response of the closed loop AVR system is:

$$v_t(t) = L^{-1} \left\{ \frac{G_{PID}(s)}{1 + G_{PID}(s)} \frac{1}{s} \right\} + 0.01 L^{-1} \left\{ \frac{G_{PID}(s)}{1 + G_{PID}(s)} \right\} \quad (46)$$

Fig.ure 7, shows the Bode plots of the open loop transfer functions $G(s) = C(s) G_P(s)$ of (38) of the proposed approach and $G_{PID}(s) = C_{PID}(s) G_p(s)$ of (44) of the approach in [25].
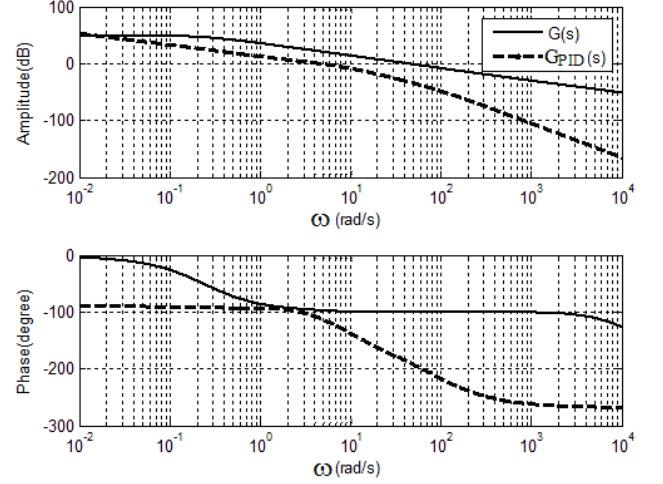
Figure 7 : Bode plots of the open loop transfer functions G(s) and $G_{PID}(s)$

From figure 7, we note that the proposed AVR system design presents a flat phase around its unity gain crossover frequency but the designed AVR system of [25] does not. We know that the flatness of the phase around its unity gain crossover frequency of the open loop transfer function of a feedback control system exhibits the so called iso-damping property of its step response which is an important robustness characteristic. Figure 8, shows the terminal voltage step responses of the closed loop AVR system of (46) with the PID controller of (43) and of the closed loop AVR system of (40) with the proposed controller of (37).
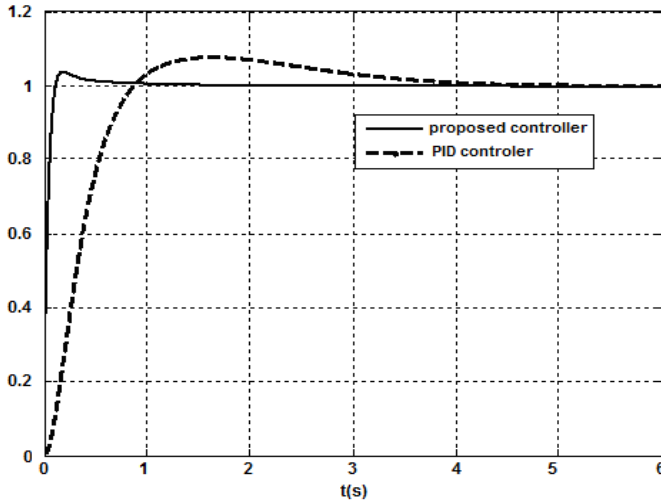

Figure 8 : The terminal voltage step response of the closed loop AVR system with the proposed controller and with the PID controller

From Fig. 8, we note that the proposed and the PID controllers achieve a small overshoot, a small settling time and a steady state error. However, the settling time of the AVR system with the proposed controller is much smaller than the one with the PID controller of [25].

In the linearized model of equation (11), the generator is represented by the gain K_g and time constant t_g. These constants are load dependent where K_g varies between 0.7 and 1.0 and τ_g between 1.0 and 2.0. Hence, to measure the robustness of the performances of the proposed AVR system design and compare them with the designed AVR system with a classical PID controller of [25], we will analyze the variations of their respective phase margins φ_m overshoots Os(%) and the settling times T_s in terms of the variations of the gain K_g and the time constant τ_g of the generator. In both closed loop AVR system designs the controllers are derived and kept unchanged in the robustness analysis for the nominal values of $K_g = 1.0$ and $\tau_g = 1.0$. To show the variations of the performances of the closed loop AVR system, the two terminal voltage step responses of the closed loop AVR system with the PID and the proposed controllers are given, respectively, in figures 9, 10 and 11, for the following three cases :

- nominal value of $K_g = 1.0$ and maximum value of $\tau_g = 2$
- nominal value of $\tau_g = 1$ s and minimum value of $K_g = 0.7$
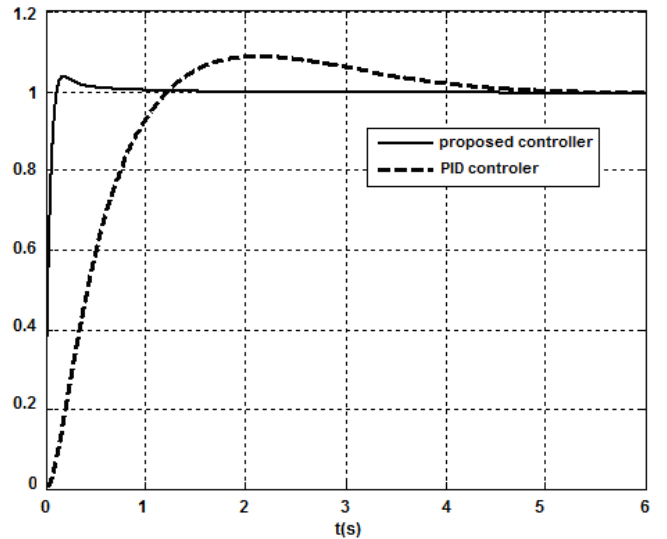- minimum value of $K_g = 0.7$ and maximum value of $\tau_g = 2$s.

Figure 9 : The terminal voltage step response of the closed loop AVR system with the PID controller and with the proposed controller for Kg = 1 and τ_g = 2 s

The obtained performance results of the overshoot Os(%) and the settling time T_s in terms of the variations of the gain K_g and the time constant τ_g of the generator for the nominal and the three above case are summarized in the table 1.

From Table 1, we note that the performance variations of the closed loop AVR system with the PID controller [25] are much larger than the ones of the closed loop AVR system with the proposed controller. This shows the effectiveness of the proposed AVR design.
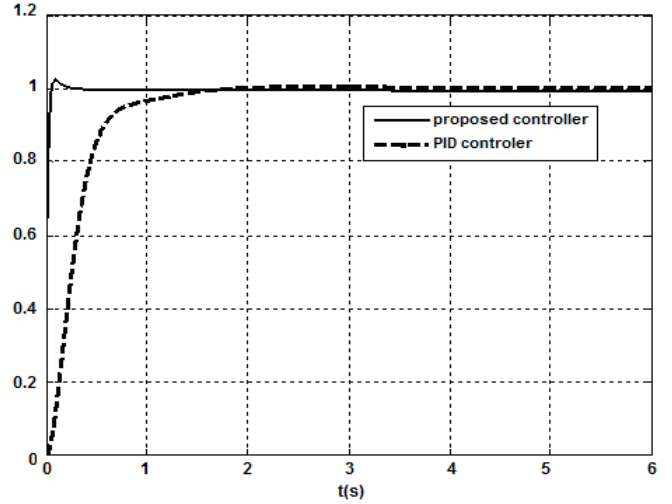
Figure 10 : The terminal voltage step response of the closed loop AVR system with the PID controller and with the proposed controller for Kg = 0.7 and τ_g = 1 s


Figure 11 : The terminal voltage step response of the closed loop AVR system with the PID controller and with the proposed controller for Kg = 0.7 and τ_g = 2 s

Table 1 : Performance results of the overshoot Os(%) and the settling time T_s

K_g and τ_g values	Proposed AVR design	PID AVR design [25]
K_g =1 and τ_g =1 (Nominal cas)	Os(%) = 2.576 Ts = 0.126	Os(%) = 0.3716 Ts = 0.990
K_g = 1 and τ_g = 2e	Os(%) = 3.755 Ts = 0.3299	Os(%) = 7.4925 Ts = 3.3506
K_g = 0.7 and τ_g = 1	Os(%) = 2.2458 Ts = 0.1613	Os(%) = 0.471 Ts = 1.256
K_g = 0.7 and τ_g = 2	Os(%) = 3.755 Ts = 0.3299	Os(%) = 8.666 Ts = 4.037

Figures 12 and 13 show, respectively, the plots of the variations of the phase margin φ_m of the closed loop AVR system versus the gain K_g and the time constant τ_g for the proposed and the classical PID controller of [25].
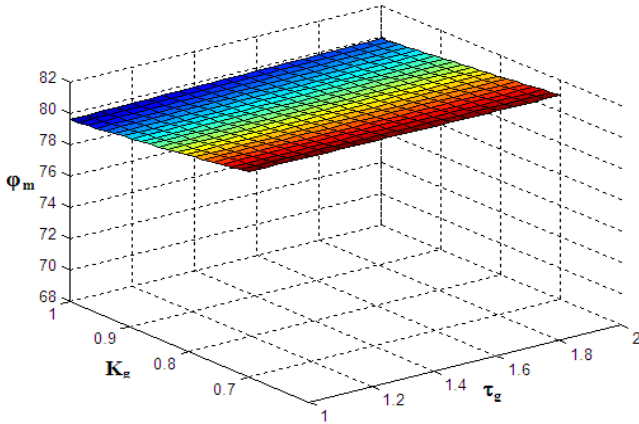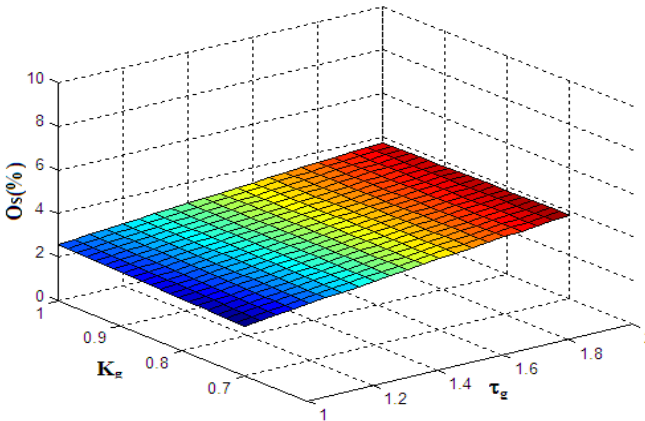

Figure 12 : Plot of the phase margin φ_m versus K_g and τ_g of the AVR system with the proposed controller
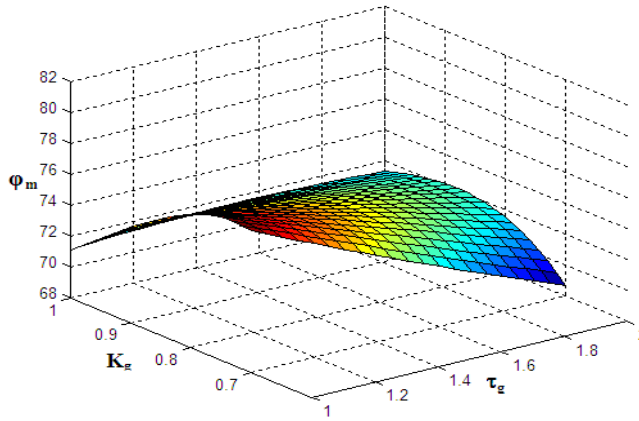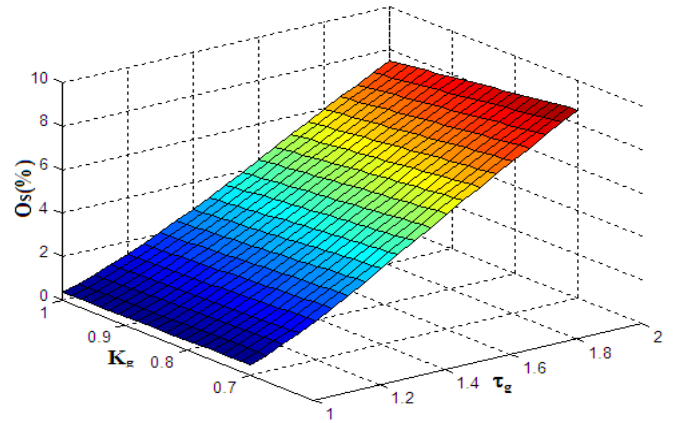

Figure 13 : Plot of the phase margin φ_m versus K_g and τ_g of the AVR system with a classical PID controller of [25]

Figures 14 and 15 show, respectively, the plots of the variations of the overshoots Os(%) of the AVR system versus K_g and τ_g for the proposed and the classical PID controller of [25].
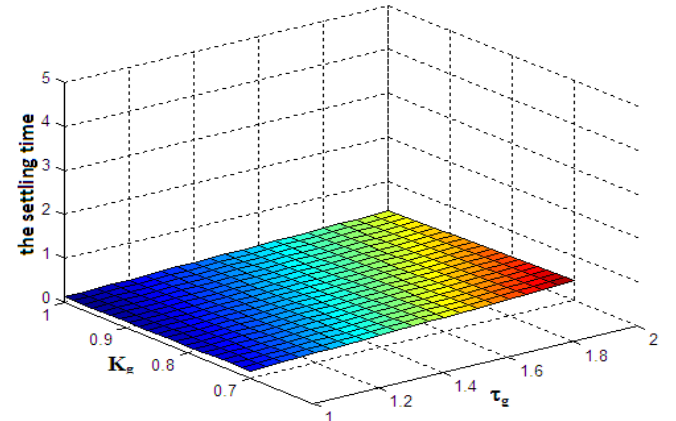

Figure 14 : Plot of the overshoot Os(%) versus K_g and τ_g of the AVR system with the proposed controller
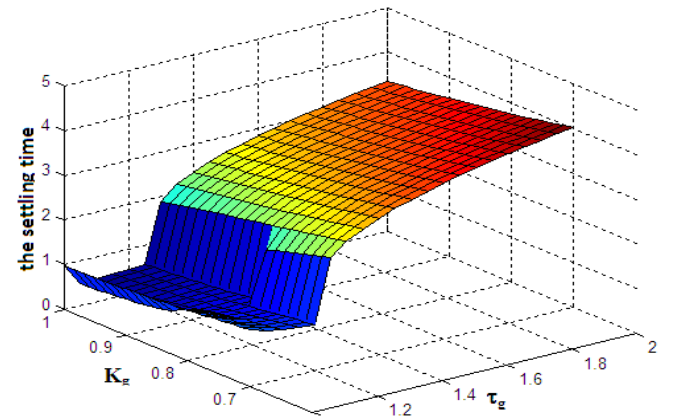

Figure 15 : Plot of the overshoot Os(%) versus K_g and τ_g of the AVR system with a classical PID controller of [25]

Figures 16 and 17 show, respectively, the plots of the variations of the settling time of the AVR system versus K_g and τ_g for the proposed and the classical PID controller of [25].

Figure 16 : Plot of the settling time versus K_g and τ_g of the AVR system with the proposed controller

Figure 17 : Plot of the settling time versus K_g and τ_g of the AVR system with a classical PID controller of [25]

From the six figures. 12-17, we clearly see that the plots of the phase margin φ_m, the overshoot Os(%) and the settling time versus the generator's gain K_g and time constant τ_g of the closed loop AVR system with the

proposed controller are completely flat and the ones of the closed loop AVR system with the classical PID controller of [25] are sloped and distorted. This means that the performances of the closed loop AVR system with the proposed controller are almost insensitive to the variations of the gain K_g and the time constant τ_g of the generator. According to these results, it can be said that the proposed closed loop AVR system is robust and provides the desired control behavior without the effect of changes of the load. Hence, the terminal voltage of the generator of the proposed closed loop AVR system is almost load independent.

CONCLUSION

In this work, a robust AVR design using fractional order control techniques has been presented. The proposed controller design strategy guarantees that the open loop transfer function of the AVR system is the Bode's ideal transfer function that is widely used in the fractional order control domain because of its iso-damping property which is an important robustness feature. The controller design process has been shown to be based on the rational function approximation of the fractional order integrator. The obtained simulations results in terms of frequency and time responses and performances analysis of the closed loop AVR system have shown the effectiveness and the usefulness of the proposed AVR system design. Comparisons are made with a PID controller and it has been clearly seen that the proposed controller can highly improve the system robustness with respect to the generator parameter's changes due to load. Then, according to these results, it can be said that the proposed closed loop AVR system is robust, provides the desired control behavior and makes the terminal voltage of the generator almost load independent.

Références

[1] A.Oustaloup, *La Commande CRONE,* Paris:Hermès, 1991.

[2] C.A. Monje, Y.Q. Chen, B.M. Vinagre, D. Xue, V. Feliu, *Fractional-Order Systems and Controls Fundamentals and Applications*, London:Springer-Verlag, 2010.

[3] R. Caponetto, G. Dongola, L. Fortuna, I. Petras, *Fractional Order Systems: Modeling and Control Applications,* Singapore: World Scientific, 2010.

[4] Y. Luo, Y.Q. Chen, *Fractional Order Motion Controls,* Chichester, United Kingdom : John Wiley & Sons Ltd, 2012.

[5] D.Valerio, J. Sa da Costa, *An Introduction to Fractional Control,* London: Institution of Engineering and Technology, 2013.

[6] I. Pan, S. Das, *Intelligent Fractional Order Systems and Control: An Introduction,* Berlin : New York, Springer, 2013.

[7] H.W. Bode, *Network Analysis and Feedback Amplifier Design,* New York: Van Nostrand, 1945.

[8] A. Tustin et al, "The Design of Systems for Automatic Control of the Psition of Massive object, " *Proceedings of Institution of Electrical Engineers,* vol. 105, no. 1, pp. 1-57, 1958.

[9] S. Manabe, "The Non-Integer Integral and its Application to Control Systems, "*ETJ of Japan,* vol. 6, no. 3-4, pp. 83-87, 1961.

[10] A. Oustaloup, *Systèmes Asservis Linéaires d'Ordre Fractionnaire: Théorie et Pratique,* Paris: Editions Masson, 1983.

[11] M. Axtell, E.M. Bise, Fractional Calculus Applications in Control Systems, *Proceedings of the IEEE Nat. Aerospace and Electronics Conf., N.Y, pp. 563–566, 1990.*

[12] I. Podlubny, "Fractional Order Systems and $PI^\lambda D^\mu$ Controllers," *IEEE Transactions on Automatic Control,* vol.44, no. 1, pp. 208-214,1999.

[13] B.M. Vinagre, I. Podlubny, L. Dorcak, V. Feliu, On Fractional PID Controllers: A Frequency Domain Approach, *In: the IFAC Workshop on Digital Control, Past, Present and Future of PID Control, , Terrasa, Spain. April 5-7, 2000.*

[14] C.A. Monje, B.M. Vinagre, Y.Q. Chen, V. Feliu, P. Lanusse, J. Sabatier, Proposals for fractional $PI^\lambda D^\mu$ tuning, *In: Proceedings of the 1st IFAC Workshop on Fractional Differentiation and its Applications, Bordeaux, France, FDA'04, July 19-21, 2004.*

[15] R. Caponetto, L. Fortuna, A new tuning Strategy for a non integer order PID Controller, *In: Proceedings of the 1st IFAC Workshop on Fractional Differentiation and its Applications, Bordeaux, France, FDA'04, July 19-21, 2004.*

[16] A. Djouambi, A. Charef, T. Bouktir, "Fractional Order Robust Control and $PI^\lambda D^\mu$ Controllers, " *WSEAS Trans. on Circuits and Systems,* vol. 4, no. 8, pp. 850-57, 2005.

[17] D. Valério, J. Sà da Costa, "Tuning of fractional PID controllers with Ziegler-Nichols type rules, " *Signal Processing,* vol. 86, pp. 2771-84, 2006.

[18] C.A. Monje, and B.M. Vinagre, V. Feliu, Y.Q. Chen, "Tuning and auto-tuning of fractional order controllers for industry applications, "*Control Engineering Practice,* vol. 16, pp. 798-12, 2008.

[19] K. Bettou, and A. Charef, "Control Quality Enhancement using Fractional $PI^\lambda D^\mu$ Controller, " *International Journal of System Sciences,* Vol. 40, no. 8, pp. 875-88, 2009.

[20] F. Merrikh-Bayat, and M. Karimi-Ghartemani, "Method for Designing $PI^\lambda D^\mu$ Stabilizers for Minimum-Phase Fractional-Order Systems, " *IET Control Theory Appl,* vol. 4, no. 1, pp. 61-70, 2010.

[21] Y.Q. Chen, I. Petras, and D. Xue, Fractional Order Control - A Tutorial, *In: Proceedings American Control Conference, St. Louis, MO, USA, pp. 1397-1411 , June 10-12, 2009.*

[22] H. Yoshida, K. Kawata, and Y. Fukuyama, "A Particle Swarm Optimization for Reactive Power and Voltage Control Considering Voltage Security Assessment, " *IEEE Trans. Power Systems*, vol. 15, pp. 1232–39, 2000.

[23] Z.L. Gaing,"A particle Swarm Optimization Approach for Optimum Design of PID Controller in AVR System," *IEEE Trans. Energy Conversion,* vol. 19, no. 2, pp. 384-91, 2004.

[24] V. Mukherjee, and S.P. Ghoshal, "Intelligent Particle Swarm Optimized Fuzzy PID Controller for AVR System," *Electric Power System Research,* vol. 77, no. 12, pp. 1689-98, 2007.

[25] L. Coelho, "Tuning of PID Controller for An Automatic Regulator Voltage System Using Chaotic Optimization Approach," *Chaos Solit. & Fractals,* vol. 39, no. 4, pp. 1504-14, 2009.

[26] H. Zhu, L. Li, Y. Zhao, Y. Guo, and Y. Yang, "CAS Algorithm-Based Optimum Design of PID Controller in AVR System," *Chaos, Solitons and Fractals,* vol. 42, pp. 792-800, 2009.

[27] D. Devaraj, and B. Selvabala,"Real-Coded Genetic Algorithm and Fuzzy Logic Approach for Real-Time Tuning of Proportional–Integral–Derivative controller In Automatic Voltage Regulator System,"*IET Generation, Transmission & Distribution,* vol. 3, no. 7, pp.641-49, 2009.

[28] H. Gozde, M. C. Taplamacioglu, and I. Kocaarslan, "Application of Artificial Bees Colony Algorithm in

Automatic Voltage Regulator (AVR) System," *International Journal on Technical and Physical Problems of Engineering (IJTPE),* vol. 1, no. 3,pp. 88-92, 2010.

[29] D.H. Kim, "Hybrid GA–BF Based Intelligent PID Controller Tuning for AVR System," *Applied Soft Computing,* vol. 11, pp. 11–22, 2011.

[30] M.N. Anwar, S. Pan, "A Frequency Domain Design of PID Controller for An AVR System," *Journal of Zhejiang University-SCIENCE,* vol. 15, no. 4, pp. 293-299, 2014.

[31] M. Zamani, M. Masoud Karimi-Ghartemani, N. Sadati, and M. Parniani, "Design of A Fractional Order PID Controller for An AVR Using Particle Swarm Optimization," *Control Engineering Practice,* vol. 17, pp. 1380–87, 2009.

[32] M.I. Alomoush, "Fractional Calculus-Based Optimal Controllers of Automatic Voltage Regulator in Power System, *Control and intelligent systems,* vol. 38, no. 1, pp. 40-48, 2010.

[33] I. Pan, and S. Das, "Chaotic Multi-Objective Optimization Based Design of Fractional Order PI$^\lambda$D$^\mu$ Controller in AVR System," *International Journal of Electrical Power & Energy Systems*, vol. 43, no.1, pp. 393-407, 2012.

[34] H. Ramezanian, S. Balochian, and A. Zarz, "Design of Optimal Fractional Order PID Controllers Using Particle Swarm Optimization Algorithm for Automatic Voltage Regulator (AVR) System," *Journal Control, Automation and Electrical Systems,* vol. 24, pp. 601-611, 2013.

[35] D.L. Zhang, Y.G. Tang, and X.P. Guan, "Optimum Design of Fractional Order PID Controller for an AVR System Using an Improved Artificial Bee Colony Algorithm," *Acta Automatica Sinica,* vol. 40, no.5, pp. 973-979,2014.

[36] I. Pan, and S. Das, "Frequency Domain Design of Fractional Order PID Controller for AVR System Using Chaotic Multi-Objective Optimization," *Electrical Power* and *Energy Systems,* vol. 51, pp.106–118, 2013.

[37] A. Djouambi, A. Charef, and A.V. Besançon, Fractional Order Controllers Based on Bode's Ideal Transfer Function," *Inter. Journal of Control and Intelligent Systems,* Vvol. 38, no. 2, pp. 67-73, 2010.

[38] R.S. Barbosa, J.A. Machado, and I.M. Ferreira, "Tuning of PID Controllers Based on Bode's Ideal Transfer Function," *Nonlinear Dynamics,* vol. 38, no.1-4, pp. 305-21, 2004.

[39] M. Assabaa, A. Charef, Z. Santouh, M. Benmalek, "Modeling and analysis of multiple fractional Order systems," *In : Proceedings de la 5ème Conférence sur le génie électrique, CGE'05, Algiers, Algeria, April 16-17, 2007.*

[40] A. Charef, "Analogue Realization of Fractional Order Integrator, Differentiator and Fractional PI$^\lambda$D$^\mu$ Controllers," *IEE proceedings on Control Theory & Applications,* vol. 153, no.6, pp. 714-20, 2006.

[41] A. Charef, "Modeling and Analog Realization of the Fundamental Linear Fractional Order Differential Equation," *Nonlinear Dynamics,* vol. 46,no. 1-2, pp. 195-210, 2006.